Quantum treatment of two-stage sub-Doppler laser cooling of magnesium atoms

O. N. Prudnikov,[1,2,*] D. V. Brazhnikov,[1,2,†] A. V. Taichenachev,[1,2] V. I. Yudin,[1,2,3] A. E. Bonert,[2] R. Ya. Il'enkov,[1,2] and A. N. Goncharov[1,2,3]

[1]*Novosibirsk State University, Novosibirsk 630090, Russia*

[2]*Institute of Laser Physics SB RAS, Novosibirsk 630090, Russia*

[3]*Novosibirsk State Technical University, Novosibirsk 630073, Russia*

(Received 1 May 2015; revised manuscript received 13 November 2015; published 15 December 2015)

Deep laser cooling of ^{24}Mg atoms has been theoretically studied. We propose a two-stage sub-Doppler cooling strategy using electrodipole transition $3\,^3P_2 \to 3\,^3D_3$ ($\lambda = 383.8$ nm). The first stage implies exploiting magneto-optical trap with σ^+ and σ^- light beams, while at the second stage lin $\perp$ lin molasses is used. We focus on achieving a large number of ultracold atoms ($T_{\rm eff} < 10\ \mu$K) in a cold-atomic cloud. The calculations have been based on quantum treatment, taking into full account the recoil effect and beyond many widely used approximations. Steady-state values of average kinetic energy and linear momentum distributions of cold atoms have been analyzed for various light-field intensities and frequency detunings. The results of conducted quantum analysis have been significantly different from the results achieved under a semiclassical approximation based on the Fokker-Planck equation. The second cooling stage allows achieving sufficiently lower kinetic energies of the atomic cloud as well as increased fraction of ultracold atoms at certain conditions compared to the first one. We hope that the obtained results can help in overcoming current experimental problems in deep cooling of ^{24}Mg atoms by means of laser field. Cold magnesium atoms cooled in a large amount to several μK are of huge interest to, for example, quantum metrology and to other many-body cold-atoms physics.

DOI: 10.1103/PhysRevA.92.063413 PACS number(s): 37.10.De, 05.10.Gg, 06.30.Ft

I. INTRODUCTION

Laser cooling and trapping of neutral atoms play an important role in many directions of modern quantum physics. For example, quantum metrology is among these directions, which has been rapidly developing in recent years. It is aimed at creating standards for physical quantities and conducting highly accurate measurements with the help of them (e.g., see [1]). Today, the most precise measurements are possible for such physical quantities as frequency and time due to success achieved in producing etalons (standards) for them. Modern time standard is based on the frequency standard, which determines its stability and accuracy to a considerable degree. Meanwhile, frequency etalons can be used not only as a basis for time standards, but also to measure precisely other physical quantities and constants such as, for instance, electrical current and voltage, magnetic field, length, the Rydberg and fine-structure constants.

High-accuracy experiments for versatile examination of relativistic and quantum theories have become feasible owing to modern frequency standards. Among practical applications of time and frequency standards, the broadband communication networks and navigational and global positioning systems should be especially mentioned. Many laboratories of world-known scientific centers conduct their studies in the field of frequency standards. One of the latest trends in this field is connected with the concept of intercity or even international quantum clock network that could combine time-keeping standards all over the world into one system [2–6].

Today, there are two main development strategies for primary frequency standards: based on the electric quadrupole ion trap and based on many neutral atoms trapped in the optical lattice (e.g., see [7,8]). The latter strategy is the most modern and has been rapidly developing. The idea of neutral atoms trapping in a periodic light potential is not new and was actively studied in the 1970s (see [9] and references therein). As for metrological purposes, this idea experienced its rebirth in the beginning of the 21st century after noticeable progress in technique and methods of laser cooling of atoms, development of the "magic"-wavelength concept [10,11], and also experimental and theoretical success in spectroscopy of forbidden atomic transitions [12–16]. Today, stability of optical lattice-based frequency standards stands practically on the same level with single-ion standards and in some cases even exceeds them. Relative instability and uncertainty of the state-of-the-art prototypes of frequency standards have reached extremely low levels 10^{-17}–10^{-18} [17–20].

Alkaline-earth and alkaline-earth-like atoms such as Yb (for instance, see [21–23]), Ca [24], Sr [18,19,25], Hg [26], and Mg [27,28] are among the main candidates to create frequency standards of a new generation. They are the most appropriate because of narrow spectroscopic lines connected with forbidden optical transitions from the ground state $^1S_0$ to the lowest excited triplet state $^3P_{0,1,2}$ (see Fig. 1). Moreover, one more key circumstance is the existence of so-called "magic" wavelength for these transitions at which the first-order light shift from optical lattice field vanishes. Also, one of the last trends is connected with spectroscopy of transition $^1S_0 \to {}^3P_0$ in even isotopes (with zero nucleus spin), which is highly forbidden. Frequency of this transition is immune to many frequency-shift effects, therefore, it can be exploited as a good "clock" transition. In spite of the fact that such transition is highly forbidden, it has already been observed by magnetic-field-induced spectroscopy [29] in ^{174}Yb [21], ^{88}Sr [25,30–32], and ^{24}Mg [33,34].

*oleg.nsu@gmail.com

†brazhnikov@laser.nsc.ru

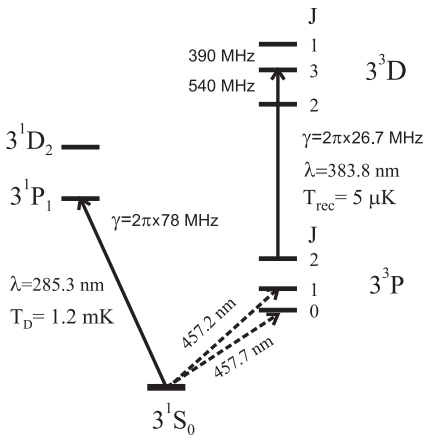

FIG. 1. Partial energy diagram of ^{24}Mg atom. Solid lines denote the cooling transitions with corresponding temperature limits, while dashed lines denote possible "clock" transitions, which can be used for laser stabilizing.

The experimental results to date have demonstrated that the first four elements (Yb, Ca, Sr, and Hg) can be effectively cooled by the laser methods to ultralow temperatures, close to the recoil energy limit, that is required for effective loading of an optical lattice (∼1–10 μK). Besides, even subrecoil temperatures can be obtained by using the evaporative cooling technique, getting the Bose-Einstein condensation [35–37]. Unfortunately, researchers have not been able to reach the same great success with Mg atoms. In particular, neither two-photon laser cooling [38] nor laser quenching [39] methods have appeared to be effective in case of magnesium. The minimum temperature of a magnesium cloud that has been obtained by laser cooling is about 500 μK, that is rather far from desirable range of values, in particular, from the recoil temperature (3–10 μK, depending on the atomic transition).

At the same time, magnesium atoms have some advantages compared to the other candidates in terms of the frequency standard. Thus, the blackbody radiation (BBR) shift is one of the main limiting factors for accuracy and stability of the quantum frequency standard (e.g., see [2,8,19]). BBR shift of the clock transition $3\,^1S_0 \rightarrow 3\,^3P_0$ for magnesium is much smaller than for Yb, Ca, Sr and just a little bit higher than for a mercury atom (see Table I). However, from the viewpoint of the experiment, Mg has some advantages against Hg. In particular, mercury atoms require noticeably smaller wavelengths for laser spectroscopy, cooling, and trapping than magnesium atoms do. For instance, an optical potential depth at the level of 50–300 in the recoil energy units is needed to effectively trap cold atoms in the nondissipative optical lattice and create the Lamb-Dicke regime (e.g., see [8,19]). It means that a highly intensive laser field at the magic wavelength λ_m should be applied. As it can be seen from Table I, λ_m(Mg) ≈ 468 nm and λ_m(Hg) ≈ 363 nm, therefore, for experimental purposes, creation of a deep optical potential for mercury atoms is a more difficult task than for magnesium atoms due to the much smaller wavelength. Aside from the relatively small BBR shift, the magnesium atom has one more advantage with respect to Ca and Sr: there is no optical pumping of atoms on the nonresonant level $3\,^1D_2$ during laser precooling stage with the help of strong dipole transition $3\,^1S_0 \rightarrow 3\,^1P_1$ (see Fig. 1) and temperatures at the level of a few mK are easy achievable [27,28,44,45].

TABLE I. Data for several atomic elements relevant for new-generation frequency standards: λ_{cl} is a wavelength of the clock transition $3\,^1S_0 \rightarrow 3\,^3P_0$ and λ_m is its magic wavelength, BBR frequency shifts are indicated with respect to absolute frequencies of clock transition (λ_{cl} is taken from NIST Atomic Spectra Database [40]). The boldface row corresponds to magnesium atom, which is considered in our paper.

Atom	λ_{cl}	λ_m	BBR shift
Sr	698.5	813.5 [12]	-5.5×10^{-15} [42]
Yb	578.4	759.4 [21,23]	-2.6×10^{-15} [42]
Ca	659.7	735.5 [24]	-2.6×10^{-15} [42]
Mg	**457.7**	**≈468** [41]	$\mathbf{-3.9 \times 10^{-16}}$ [42]
Hg	265.6	362.6 [26]	-2.4×10^{-16} [15,43]

Recent experiments [33,34,46] showed some noticeable progress in cooling of ^{24}Mg atoms. The atoms were cooled down to the record temperature equaled to 1.3 μK and confined in an optical lattice. However, the final number of atoms was about 10^4 that made approximately 0.01% of the initial number of atoms in the magneto-optical trap (MOT) based on the cyclic triplet dipole transition $3\,^3P_2 \rightarrow 3\,^3D_3$. That great loss in atomic number was due to the fact that atomic velocity selection (roughly speaking, similar to evaporative cooling method) was used to reach such ultralow temperature, but laser cooling in the MOT, unfortunately, showed the cloud temperature equaled to about 1 mK. That result lagged significantly behind the successful results achieved with other elements (Ca, Sr, Yb, Hg). However, we believe that improved strategy of laser cooling of magnesium atoms may allow getting much better results of laser-cooling temperature as well as the number of atoms trapped.

Therefore, we can state that the problem of deep cooling of magnesium atoms by laser radiation is still unsolved. Moreover, increasing ultracold atomic number has principal importance for many applications of cold atoms. For instance, authors of the paper [47] managed to obtain the Bose-Einstein condensation composed of ∼10^7 strontium atoms. Besides, frequency-standard stability increases with increasing number of atoms in an optical lattice [1,48]. All things considered, we can conclude that it is important to solve the problem of deep laser cooling of magnesium atoms (down to T∼1–10 μK) as well as to provide a much larger number of ultracold atoms in a lattice.

II. LASER COOLING IN A MOT: SEMICLASSICAL APPROXIMATION

Laser cooling of neutral atoms in a magneto-optical trap is one of the main cooling methods. The laser field composed of six beams with orthogonal circular polarizations ($\sigma^+\sigma^-$ configuration) was suggested in [49] as an effective way to cool and trap atoms simultaneously. Narrow spectral lines allow laser cooling of various atoms down to a few tens and units of μK, and even lower. In particular, narrow intercombination transition $4\,^1S_0 \rightarrow 4\,^3P_1$ in ^{40}Ca ($\gamma \approx 2\pi \times 400$ Hz) provides

temperatures around 4–6 μK [50,51] just with the help of Doppler cooling technique. Exploiting intercombination transitions showed also good results with other elements: Sr [52], Yb [21,53], and Hg [43], both for even and odd isotopes. In some extent, even isotopes, having a zero nuclear spin, are more attractive for frequency standards of a new generation, based on cold atoms trapped in a three-dimensional (3D) optical lattice. However, as it has been already mentioned in the Introduction, still no satisfactory results of cooling ^{24}Mg atoms by means of laser radiation have been observed in contrast to the other elements.

We tried to solve the problem with deep laser cooling of magnesium in the recent work [54], where the detailed theoretical study of magnesium kinetics in the one-dimensional (1D) MOT using the dipole transition $3\,^3P_2 \to 3\,^3D_3$ was conducted. The theory was based on the widely used semiclassical approach [9,55], based on the well-known assumptions

$$\omega_{\rm rec} \ll \min\{\gamma, \gamma S\} \tag{1}$$

and

$$\Delta p \gg \hbar k\,. \tag{2}$$

Here, $\omega_{\rm rec} = \hbar k^2/2M$ is the recoil frequency, M is mass of an atom, $k = 2\pi/\lambda$ is wave number. The saturation parameter S is defined as

$$S = \frac{R^2}{(\gamma/2)^2 + \delta^2}\,, \tag{3}$$

where γ is the spontaneous relaxation rate of excited state, $\delta = \omega - \omega_0$ is detuning of laser radiation frequency ω from the transition frequency ω_0, and R is the Rabi frequency.

Condition (1) implies that recoil frequency must be rather small in comparison with a typical rate of steady state settling among atomic internal degrees of freedom. In particular, in case of an atom without any degeneracy of the ground state, this rate is defined by γ. If there is a degenerate ground state, and optical pumping can occur, this rate is defined by γ or the pumping rate γS, depending on what is smaller. The second semiclassical requirement (2) implies that typical width of stationary linear momentum distribution $f(p)$ must be significantly larger than the recoil momentum from emission and absorption of a photon.

Doppler limit for temperature of laser cooling T_D, achieved at the frequency detuning $\delta = -\gamma/2$, can be figured out from equation for minimum kinetic energy in the one-dimensional case

$$E_{\rm kin}^{\rm min} = \frac{1}{2}k_B T_D = \frac{7}{40}\hbar\gamma. \tag{4}$$

Strictly speaking, this equation is valid for transition $J_g = 0 \to J_e = 1$. It was found in [56] under $\sigma^+\sigma^-$ configuration (also see [57]). If we use this formula to estimate T_D in case of transition $3\,^3P_2 \to 3\,^3D_3$ ($\gamma \approx 2\pi 26.7$ MHz), we immediately find $T_D \approx 425\,\mu$K. To trap atoms effectively with such relatively high temperature, the large intensity of continuous wave (cw) optical lattice field at the level of tens of MW/cm^2 would be required, which is hardly feasible in the experiment. Therefore, much lower temperature of the atomic cloud is needed. At the same time, since the considered transition has degenerate energy levels, it is possible to anticipate so-called sub-Doppler mechanism to be activated during laser cooling in a MOT under the polarization-gradient field. In principle, this process would overcome the Doppler limit (4) and show much lower temperature than in the case of $J_g = 0 \to J_e = 1$.

A semiclassical approach is based on a kinetic equation of Fokker-Planck type for the Wigner distribution function in phase space $f(z,p)$. That equation can be derived by reducing the exact quantum kinetic equation for the density matrix by decomposition technique on small parameter $\hbar k/\Delta p \ll 1$ to the second-order terms. This procedure is well known and it has been used by many authors (e.g., see [58–61]). Eventually, the following equation can be obtained:

$$\frac{p}{M}\frac{\partial}{\partial z} f(z,p) = \left[-\frac{\partial}{\partial p}F(z,p) + \frac{\partial^2}{\partial p^2}D(z,p)\right] f(z,p). \tag{5}$$

Here, $F(z,p)$ is the laser-field force that affects the atom, $D(z,p)$ is atom diffusion in the laser field. This equation must be completed with the normalizing condition that in one-dimensional periodic laser field has the following form:

$$\frac{1}{\lambda}\int_{-\lambda/2}^{+\lambda/2} dz \int_{-\infty}^{+\infty} f(p,z)dp = 1.$$

One-dimensional $\sigma^+\sigma^-$ laser-field configuration allows significant simplifying of the formula (5), thus, the dependence f on z vanishes (see Sec. III B).

Our semiclassical calculations [54] have been done beyond many widely used approximations (for instance, slow atoms and weak-field approximations). As it has been shown, the minimum kinetic energy achievable in the MOT is close to $30E_{\rm rec}$, where $E_{\rm rec} = \hbar\omega_{\rm rec}$ is recoil energy. The effective temperature, which can be associated to this value, is $T_{\rm eff} \approx 150\,\mu$K. It is approximately three times lower than the Doppler limit $T_D \approx 425\,\mu$K, but, unfortunately, it is still very far from desirable range of values and, in particular, the recoil temperature $T_{\rm rec} = 5\,\mu$K.

Let us consider the question of the applicability of semiclassical approach to the magnesium problem. Indeed, as it will be shown further, on the basis of 1D semiclassical treatment, the optimal parameters of cooling field for transition $3\,^3P_2 \to 3\,^3D_3$ can be chosen as $\delta = -2\pi \times 130$ MHz and $I = 500$ mW/cm^2. The corresponding saturation parameter $S \approx 4 \times 10^{-2}$. In spite of such low saturation, the first semiclassical requirement (1) seems to be satisfied since $\omega_{\rm rec} = 2 \times 10^{-3}\,\gamma$ (see also Sec. III D). At the same time, typical momentum distribution width Δp may not satisfy the second semiclassical condition (2). Indeed, in general the momentum distribution of atoms can be complicated. In particular, Fig. 2 shows two examples of momentum distributions for different values of the light-field intensity. The distribution has bimodal profile at low intensity $I = 20$ mW/cm^2: there is the high-contrast spike on top of the wide background. This background conditionally describes "hot" fraction of atoms in a cloud with effective temperature $T_{\rm eff} \sim$ 1–10 mK, while the spike corresponds to the ultracold fraction with $T_{\rm eff} \sim 1\,\mu$K. Similar distributions were observed earlier (e.g., see [62] with semiclassical low-saturation-limited calculations of Sisyphus cooling of Cs atoms involved transition $F_g = 4 \to F_e = 5$ or the quantum-treatment calculations for atomic W-type

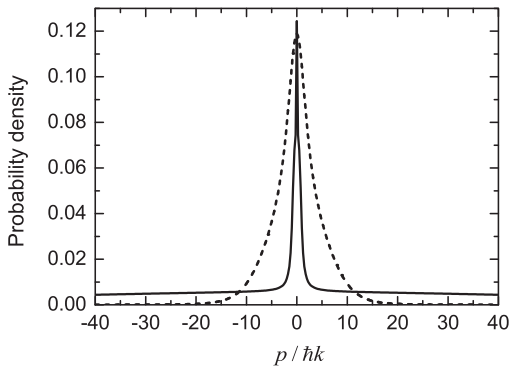

FIG. 2. Momentum distributions of magnesium atoms at $\delta = -5\gamma \approx -2\pi \times 130$ MHz, $I = 20$ mW/cm^2 (solid line), and $I = 470$ mW/cm^2 (dashed line).

scheme in [63]). In our case, the narrow-spike width is about $\hbar k$, and the requirement $\Delta p \gg \hbar k$ is not satisfied at all. With increasing intensity ($I = 470$ mW/cm^2) bimodal profile disappears. However, the distribution as a whole is still sufficiently narrow, and the second requirement (2) is not satisfied with a good margin. Also, it should be noted that the condition (2), as a matter of fact, depends on the value of the total angular momentum F_g. In other words, at the same saturation parameter S the requirement (2) will be satisfied for a small value of F_g and not be satisfied with its increasing.

In view of the aforesaid, we can conclude that more precise theoretical treatment is needed in case of magnesium to adequately describe its kinetics under laser field. The treatment can be based on the kinetic equation on the density matrix with a full view of the recoil effect (e.g., see [9,58,64]). Moreover, as it will be described in the next section, the quantum-treatment results noticeably differ from the semiclassical ones, based on Eq. (5). That difference, in particular, gave us an idea to exploit the second stage of sub-Doppler laser cooling for getting the desirable results.

III. FULL ACCOUNT OF THE RECOIL EFFECT

Let us consider the problem of magnesium atoms laser cooling beyond the semiclassical approximation as well as beyond some other widely used approximations (weak-saturation limit, secular approximation, etc.).

A. Problem statement

We assume the laser field to be one dimensional, composed of two plane monochromatic counterpropagating light waves with equal frequencies and amplitudes (the quantization axis z is collinear to the wave vectors):

$$\begin{aligned}\mathbf{E}(z,t) &= E_0\mathbf{e}_1 e^{-i(\omega t-kz)} + E_0\mathbf{e}_2 e^{-i(\omega t+kz)} + \text{c.c.}\\ &= E_0\mathbf{e}(z)\, e^{-i\omega t} + \text{c.c.},\end{aligned} \tag{6}$$

where $\mathbf{e}_{1,2}$ are the unit complex vectors of waves' polarizations, while $\mathbf{e}(z)$ is the following complex vector:

$$\mathbf{e}(z) = \mathbf{e}_1 e^{ikz} + \mathbf{e}_2 e^{-ikz}. \tag{7}$$

Nonzero components of the vectors $\mathbf{e}_{1,2}$ in the spherical basis are

$$\begin{aligned} e_1^{-1} &= -\sin(\varepsilon_1 - \pi/4),\ e_1^{+1} = -\cos(\varepsilon_1 - \pi/4),\\ e_2^{-1} &= -\sin(\varepsilon_2 - \pi/4)\, e^{i\varphi},\\ e_2^{+1} &= -\cos(\varepsilon_2 - \pi/4)\, e^{-i\varphi}.\end{aligned} \tag{8}$$

Here, $\varepsilon_{1,2}$ are the ellipticity parameters (in particular, $\varepsilon = \pm\pi/4$ corresponds to right- or left-circular polarized wave, $\varepsilon = 0$ is for linear polarization), φ is the angle between main axes of polarization ellipses. For instance, the case with $\varepsilon_{1,2} = 0$ and $\varphi = \pi/2$ corresponds to lin $\perp$ lin field configuration.

Here, quantum treatment of atomic kinetics under the laser field (6) is based on the equation on single-atom density matrix in coordinate two-point representation that has the form (e.g., see [9,55,64])

$$\frac{\partial\widehat{\rho}(z_1,z_2,t)}{\partial t} = -\frac{i}{\hbar}[\widehat{H}(z_1,t)\,\widehat{\rho} - \widehat{\rho}\,\widehat{H}(z_2,t)] + \widehat{\Gamma}\{\widehat{\rho}\}, \tag{9}$$

with the Hamiltonian

$$\widehat{H}(z_i,t) = \left(\widehat{p}_i^{\,2}/2M\right) + \widehat{H}_0 + \widehat{V}(z_i,t). \tag{10}$$

The first term in the Hamiltonian is the operator of kinetic energy of an atom ($\widehat{p}_i$ is the linear momentum operator), $\widehat{H}_0$ describes intratomic degrees of freedom, operator $\widehat{V}$ corresponds to the atom-field dipole interaction, and the linear operator functional $\widehat{\Gamma}\{\dots\}$ is responsible for relaxation processes in an atom. Let us introduce the projection operator onto the excited atom state

$$\widehat{P}^e = \sum_{m_e} |F_e,m_e\rangle\langle F_e,m_e|, \tag{11}$$

and the Wigner vector operator $\widehat{\mathbf{T}}$, whose spherical components are

$$\widehat{T}_\sigma = \sum_{m_e,m_g} C^{F_e,m_e}_{F_g,m_g;1\sigma}|F_e,m_e\rangle\langle F_g,m_g|, \tag{12}$$

with $\sigma = 0,\ \pm 1$ and $C^{F_e,m_e}_{F_g,m_g;1\sigma}$ the Clebsch-Gordan coefficients (e.g., see [65]). Then, the terms $\widehat{H}_0$ and $\widehat{V}$ from (10) in the resonant approximation can be written as

$$\widehat{H}_0 = -\hbar\delta\,\widehat{P}^e \tag{13}$$

and

$$\widehat{V}(z_i) = -\hbar R\,\widehat{\mathbf{T}}\cdot\mathbf{e}(z_i) + \text{H.c.} = -\hbar R\,\widehat{V}^{eg}(z_i) + \text{H.c.} \tag{14}$$

Here, $R = E_0 d/\hbar$ is the Rabi frequency (d is the reduced matrix element of dipole operator of an atom), $\widehat{V}^{eg}(z_i) = \widehat{\mathbf{T}}\cdot\mathbf{e}(z_i)$ is the dimensionless operator of atom-field interaction, depending on the coordinate in the general case, H.c. means Hermitian-conjugate term.

We introduce new coordinates

$$z = k(z_1 + z_2)/2, \quad q = k(z_1 - z_2), \tag{15}$$

in which the spontaneous relaxation operator from (9) has the following form:

$$\widehat{\Gamma} = -\frac{\gamma}{2}(\widehat{P}^e\widehat{\rho} + \widehat{\rho}\widehat{P}^e) + \gamma\sum_{\sigma=0,\pm1}\zeta_\sigma(q)\widehat{T}_\sigma^\dagger\rho\widehat{T}_\sigma\,, \tag{16}$$

with

$$\zeta_{\pm1} = \frac{3}{2}\left[\frac{\sin(q)}{q} - \frac{\sin(q)}{q^3} + \frac{\cos(q)}{q^2}\right],$$
$$\zeta_0 = 3\left[\frac{\sin(q)}{q^3} - \frac{\cos(q)}{q^2}\right]. \quad (17)$$

Note that without recoil effect, i.e., in the limit $q \to 0$, we have $\zeta_\sigma = 1$.

The density matrix can be divided into four matrix blocks:

$$\widehat{\rho} = \begin{pmatrix} \widehat{\rho}^{gg} & \widehat{\rho}^{ge} \\ \widehat{\rho}^{eg} & \widehat{\rho}^{ee} \end{pmatrix}. \quad (18)$$

Matrix blocks $\widehat{\rho}^{gg}$ and $\widehat{\rho}^{ee}$ describe populations of ground and excited states as well as low-frequency (Zeeman) coherences. Blocks $\widehat{\rho}^{ge}$ and $\widehat{\rho}^{eg}$ are responsible for optical coherences. Using all introduced notations in new coordinates (15), new equations on the density matrix blocks can be easily derived from Eq. (9). So, in the steady state we have the following:

$$-2i\omega_r \frac{\partial^2}{\partial q \partial z}\widehat{\rho}^{gg}(z,q) = \gamma \sum_{\sigma=0,\pm1} \zeta_\sigma(q)\widehat{T}_\sigma^\dagger \rho \widehat{T}_\sigma + iR\left[\widehat{V}^{eg\,\dagger}\left(z+\frac{q}{2}\right)\widehat{\rho}^{eg} - \widehat{\rho}^{ge}\widehat{V}^{eg}\left(z-\frac{q}{2}\right)\right], \quad (19)$$

$$\left(\gamma - 2i\omega_r \frac{\partial^2}{\partial q \partial z}\right)\widehat{\rho}^{ee}(z,q) = iR\left[\widehat{V}^{eg}\left(z+\frac{q}{2}\right)\widehat{\rho}^{ge} - \widehat{\rho}^{eg}\widehat{V}^{eg\,\dagger}\left(z-\frac{q}{2}\right)\right], \quad (20)$$

$$\left(\frac{\gamma}{2} + i\delta - 2i\omega_r \frac{\partial^2}{\partial q \partial z}\right)\widehat{\rho}^{ge}(z,q) = iR\left[\widehat{V}^{eg\,\dagger}\left(z+\frac{q}{2}\right)\widehat{\rho}^{ee} - \widehat{\rho}^{gg}\widehat{V}^{eg\,\dagger}\left(z-\frac{q}{2}\right)\right], \quad (21)$$

$$\left(\frac{\gamma}{2} - i\delta - 2i\omega_r \frac{\partial^2}{\partial q \partial z}\right)\widehat{\rho}^{eg}(z,q) = iR\left[\widehat{V}^{eg}\left(z+\frac{q}{2}\right)\widehat{\rho}^{gg} - \widehat{\rho}^{ee}\widehat{V}^{eg}\left(z-\frac{q}{2}\right)\right]. \quad (22)$$

These equations make a basis for further theoretical analysis. For instance, probability density of atomic distribution in the momentum space can be found by the formula

$$f(p) = \frac{1}{(2\pi)^2}\int_{-\infty}^{+\infty} dq \int_{-\pi}^{\pi} dz\, \mathrm{Tr}\{\widehat{\rho}(z,q)\}e^{-ipq}. \quad (23)$$

Here, the linear momentum of an atom is evaluated in the recoil momentum units $\hbar k$ and Tr[...] denotes the trace operation. Momentum distribution $f(p)$ must be normalized:

$$\int_{-\infty}^{+\infty} f(p)dp = 1. \quad (24)$$

This means that the set of equations (19)–(22) must be supplemented with the condition

$$\frac{1}{2\pi}\int_{-\pi}^{\pi} \mathrm{Tr}\{\widehat{\rho}(z,q=0)\}dz = 1. \quad (25)$$

Average kinetic energy of an atom in terms of recoil energy can be evaluated, for instance, with the help of the following formula:

$$E_k = \int_{-\infty}^{+\infty} p^2 f(p)dp. \quad (26)$$

B. First stage: Cooling in a MOT

Let us assume the atoms to be localized in a weak magnetic field region of a trap (near the trap's center). Therefore, magnetic field does not affect significantly the temperature of a cloud, and we omit it here. In other words, we consider kinetics of atoms in 1D laser field, composed of two counterpropagating beams with orthogonal circular polarizations ($\sigma^+\sigma^-$ configuration). Then, we can take $\varepsilon_1 = \pi/4$, $\varepsilon_2 = -\pi/4$, $\varphi = 0$ in Eq. (8), and polarization vector of the total light field in spherical basis takes the following form:

$$\mathbf{e}(z_i) = \mathbf{e}_{-1}e^{-ikz_i} - \mathbf{e}_{+1}e^{ikz_i}. \quad (27)$$

This form corresponds to the laser field with linear polarization, which rotates by the angle $\alpha = -kz_i$ during propagation along the z axis. At that the dimensionless operator $\widehat{V}^{eg}$ from (14) is

$$\widehat{V}^{eg}(z_i) = \widehat{T}_{-1}e^{-ikz_i} - \widehat{T}_{+1}e^{ikz_i}. \quad (28)$$

The considered field configuration has some unique features. First of all, the field has homogeneous intensity (it does not depend on z coordinate). Second, the field polarization also can be made homogeneous (e.g., see [63,66]). Indeed, let us pass to the new coordinate system K', in which the z' axis coincides with z axis in the old K system, while the axes x' and y' rotate around the z axis by the angle $\alpha = -z = -k(z_1+z_2)/2$ (see Fig. 3). In the K' system, the linearly polarized total-field vector does not rotate anymore (without loss of generality it can be considered to be directed along the x' axis). Then, in the new system the interaction operator $\widehat{V}^{eg}$ from (14) does not depend on the coordinate z_i:

$$\widehat{V}^{eg}(z_1) \Longrightarrow \widehat{V}_1(q) = \widehat{T}_{-1}e^{-iq/2} - \widehat{T}_{+1}e^{iq/2}, \quad (29)$$

$$\widehat{V}^{eg}(z_2) \Longrightarrow \widehat{V}_2(q) = \widehat{V}_1^*(q). \quad (30)$$

Since the relaxation operator $\widehat{\Gamma}$ from (16) also does not depend on z, the density matrix in the new coordinate system is not the function of z and it depends only on the q coordinate. This circumstance significantly simplifies numerical evaluations of the density matrix equations.

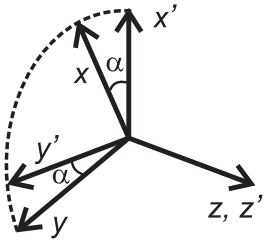

FIG. 3. Transformation the old coordinate frame K to the new one K'.

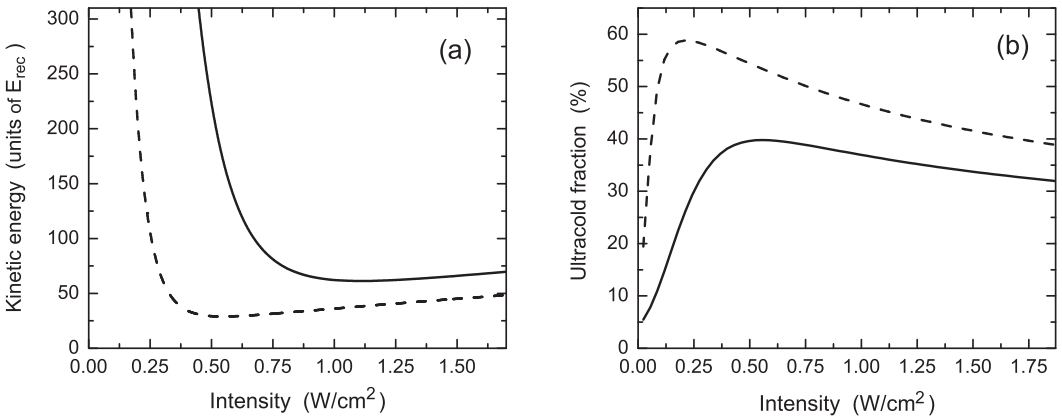

FIG. 4. Comparison of the results of semiclassical (dashed line) and quantum (solid line) treatments at $\delta = -5\gamma \approx -2\pi \times 130\,\mathrm{MHz}$. (a) Average kinetic energy of an atom as the function of light-field intensity, (b) ultracold fraction of atoms in a cloud.

The operator of rotation $\widehat{D}(\mathbf{n},\alpha)$ can be exploited to get the equations on density matrix in the new basis (e.g., see [65]). Here, the unit vector $\mathbf{n}$ defines a rotation axis, while α is a rotation angle. In our case, it is natural to coincide $\mathbf{n}$ with quantization axis z and take $\alpha = -z$. Then, influence of the rotation operator on the wave function $|F_a,m_a,z_i\rangle$ reduces to the simple multiplication by $e^{im\alpha}$, i.e.,

$$\widehat{D}(\mathbf{n},\alpha)|F_a,m_a,z_i\rangle = e^{im_a\alpha}|F_a,m_a,z_i\rangle, \tag{31}$$

with $(a = e,g)$. In the system K' the set of equations (19)–(22) takes the following form:

$$2\omega_r \frac{\partial}{\partial q}[\widehat{F}_z,\widehat{\rho}(q)] = \widehat{\Gamma}\{\widehat{\rho}(q)\} + i\delta[\widehat{P}^e,\widehat{\rho}] + iR\,[\widehat{V}_1(q)\widehat{\rho} - \widehat{\rho}\widehat{V}_2(q)]. \tag{32}$$

At that the normalizing condition (25) becomes rather simple:

$$\mathrm{Tr}\{\widehat{\rho}(q=0)\} = 1. \tag{33}$$

Figure 4(a) shows average kinetic energy of an atom as the function of light-field intensity, calculated on the basis of numerical solution of Eq. (32). Analogical dependence is also presented, which was gained by applying semiclassical approach on the basis of Fokker-Planck equation (5). Figure 4(a) shows that the semiclassical approach (dashed line) gives the minimum kinetic energy of an atom at the level of $E_{\min} \approx 30E_{\mathrm{rec}}$, that is several times smaller than the Doppler limit $E_D \approx 87.5E_{\mathrm{rec}}$. At the same time, the quantum approach (solid line) shows the result for energy just a little bit smaller than the Doppler limit ($E_{\min} \approx 62E_{\mathrm{rec}}$). Hence, the quantum treatment of the problem demonstrates that it is hardly possible to cool magnesium atoms in a MOT down to desirable range of temperatures on the basis of transition $3\,^3P_2 \to 3\,^3D_3$. All this agrees with the experiments of research group from the University of Hannover [33,34,46]. Effective temperature corresponding to the minimum at the plot $E(I)$ for the quantum-treatment result is about 310 μK at frequency detuning $\delta = -5\gamma \approx -2\pi \times 130\,\mathrm{MHz}$ and the light-field intensity $I \approx 1100\,\mathrm{mW/cm^2}$.

Aside from the temperature of an atomic ensemble, it is also important to consider the profile of momentum distribution of atoms in a cloud. It may be found very useful, in particular, for velocity-selection "cooling" to achieve ultralow temperatures ($\sim$1 μK). Let us consider a group of atoms in the momentum space with $p \leqslant 3\,\hbar k$. Figuratively speaking, we call this fraction "ultracold." Figure 4(b) shows the number of atoms in the ultracold fraction N_c as the function of light-field intensity I. The figure shows there is a maximum near $500\,\mathrm{mW/cm^2}$. It should be noted that position of this optimum is not immediately the same as for the minimum of the dependence $E_{\mathrm{kin}}(I)$. Figure 4(b) demonstrates that about 40% of atoms can be concentrated in the ultracold fraction. For comparison, analogical dependence is presented, calculated on the basis of semiclassical approach (dashed line), which lies noticeably higher than the former one. The dependencies $E_{\mathrm{kin}}(I)$ and $N_c(I)$ lose to the semiclassical ones because quantum treatment provides significantly different results for the momentum distribution in the vicinity of $p \approx 0$. Indeed, Fig. 5 shows a very sharp spike in the semiclassical case and a tiny peak as the result of quantum calculations.

C. Second stage: Cooling in an optical molasses

Fortunately, solution of the problem of deep laser cooling of magnesium atoms can be found by involving the second

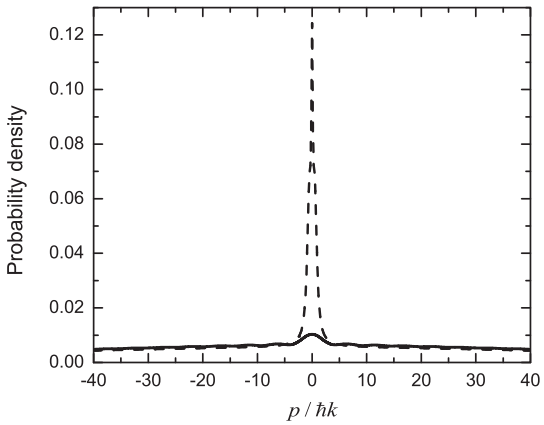

FIG. 5. Momentum distributions of magnesium atoms: comparison of semiclassical (dashed line) and quantum (solid line) treatments $\delta = -5\gamma$, $R \approx 0.22\gamma$ ($I \approx 20\,\mathrm{mW/cm^2}$).

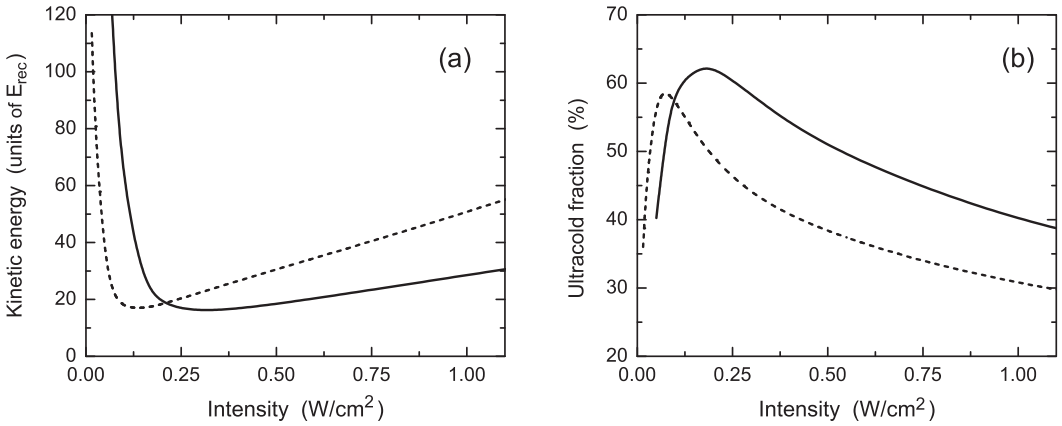

FIG. 6. (a) Average kinetic energy of an atom under lin ⊥ lin light-field configuration calculated on the basis of quantum treatment, (b) ultracold fraction of atoms in a cloud. Light-field detunings are $\delta = -2\gamma$ (dashed line) and $\delta = -5\gamma$ (solid line).

stage of sub-Doppler cooling with the help of one-dimensional optical molasses. The molasses is composed of two counter-propagating light waves with orthogonal linear polarizations (lin ⊥ lin configuration).

In contrast to $\sigma^+\sigma^-$ configuration, in the case of lin ⊥ lin field the total-field polarization transforms from linear to circular (and back) along the z axis (e.g., see [63]). Consequently, there is no rotating transformation of coordinate frame K that would make density matrix independent of the z coordinate. Therefore, we must solve the set of equations (19)–(22) on matrix $\widehat{\rho}(z,q)$. We have solved the equation numerically on the basis of the matrix continued fractions. The details of the method can be found, for example, in [64] and we do not reproduce it here. Instead of that, we just present the numerical results.

Figure 6(a) demonstrates much lower minimum kinetic energy than in case of $\sigma^+\sigma^-$ field [see Fig. 4(a), solid line). In particular, the minimum corresponds to $E \approx 16E_{\rm rec}$ at $I \approx 300$ mW/cm^2 ($T_{\rm eff} \approx 80$ μK). Besides, Fig. 6(b) shows that ultracold fraction of atoms under lin ⊥ lin light field can be higher than in case of $\sigma^+\sigma^-$ [compared to Fig. 4(b)]. The narrow structure in momentum profile near $p \approx 0$ becomes more visible than under $\sigma^+\sigma^-$ field (compare Figs. 7 and 5, solid lines). Therefore, the second cooling stage involving optical molasses can provide lower temperature as well as a larger number of atoms in ultracold fraction (up to 60%). After the second sub-Doppler cooling stage atoms may be loaded, for instance, to a shallow dipole trap. At that, a "hot" fraction of atoms (the wide background at Fig. 7) can be moved away by proper choice of the light potential depth, saving only the ultracold fraction in the trap with effective temperature $\sim$1 μK (stage of atomic velocity selection). It should be noted that implementation of the second sub-Doppler stage should eventually provide a much larger number of ultracold atoms in a dipole trap (or an optical lattice) after velocity selection in comparison with the case without the second sub-Doppler stage.

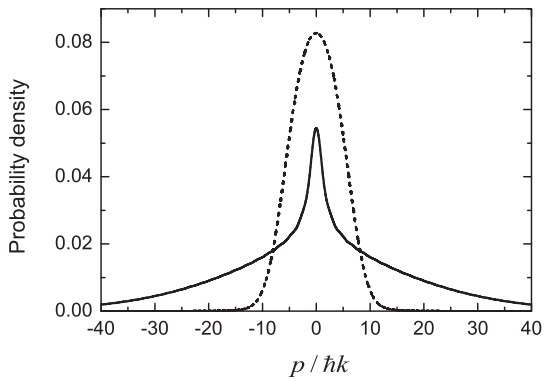

FIG. 7. Quantum calculations of momentum distributions at $\delta = -5\gamma$. Field strengths: $R \approx 0.22\gamma$, $I \approx 20$ mW/cm^2 (solid line) and $R \approx 1.13\gamma$, $I \approx 600$ mW/cm^2 (dashed line).

D. Semiclassical remarks on laser cooling under $\sigma^+\sigma^-$ and lin ⊥ lin laser fields

Let us provide here some qualitative explanation of noticeable difference in achievable kinetic energy of atoms due to laser cooling under $\sigma^+\sigma^-$ and lin ⊥ lin field's configurations. Indeed, Figs. 4(a) and 6(a) (solid lines) show optical molasses demonstrates much lower temperatures than in case of $\sigma^+\sigma^-$ field in a MOT. It is well known that these two configurations of laser field provide absolutely different mechanisms of sub-Doppler cooling, which has been theoretically and experimentally studied in details in many papers (see, for instance, [63]). In our case, we can state that sub-Doppler mechanism under $\sigma^+\sigma^-$ field almost does not work. Here, we give a qualitative explanation using semiclassical concept of radiation force.

In the regime of sub-Doppler cooling (within low-saturation limit $S \ll 1$), the light force has a dispersionlike profile (see Fig. 8). In vicinity of small atomic velocities

$$kv \ll \gamma S \tag{34}$$

radiation force is a linear function of Doppler shift kv. So, for slow atoms this force can be treated as effective friction force with friction coefficient ξ. Slope of the friction-force profile near $kv \approx 0$ is defined by sub-Doppler cooling mechanism [63]. Otherwise, at large atomic velocities regular Doppler mechanism is put in action. This cooling process occurs due to disbalance of spontaneous radiation forces from two

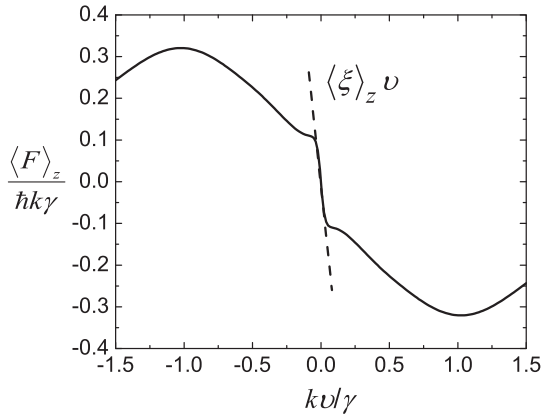

FIG. 8. Force of radiation pressure affecting atoms with transition $J_g = 2 \to J_e = 3$ under one-dimensional $\sigma^+\sigma^-$ laser field configuration. Frequency detuning is $\delta = -5\gamma$, saturation parameter is $S_0 = 0.2$. Linear approximation for slow atoms is denoted by dashed line (friction force).

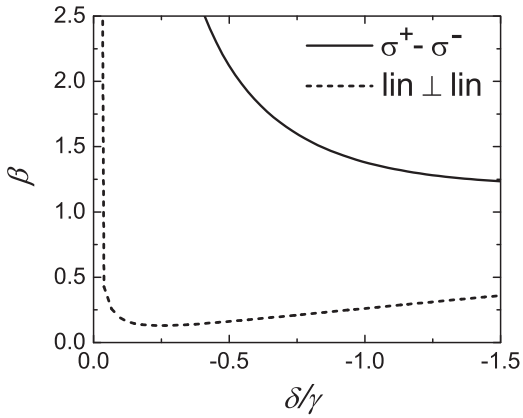

FIG. 9. Semiclassical estimation of sub-Doppler cooling temperature in units of $\hbar\gamma S_0/k_B$ for atoms with transition $J_g = 2 \to J_e = 3$ under the condition (34). Solid line is for $\sigma^+\sigma^-$ laser field configuration and dashed line is for lin $\perp$ lin one.

counterpropagating waves (see, for example, [9]). In particular, neglecting localization effects of atoms under heterogeneous optical potential of a laser field one can figure out that for slow-atoms condition steady-state velocity distribution of atoms is represented by simple Gaussian profile (see, for instance, Refs. [9,55] and Ref. [54]). Shape of this profile is defined by temperature as the ratio $\langle D \rangle_z$ to $\langle \xi \rangle_z$. Here, D is diffusion coefficient independent on atomic velocity, $\langle \dots \rangle_z$ means averaging over space coordinate z. Eventually, under low-saturation limit temperature is linearly proportional to saturation parameter

$$k_B T = \hbar\gamma\beta S_0, \tag{35}$$

where β is the dimensionless function of frequency detuning δ, S_0 is the saturation parameter (3) at exact resonance condition $\delta = 0$. Function β in significant manner depends on the light-field configuration. In cases of optical atomic transitions $J_g = 1/2 \to J_e = 3/2$ under lin $\perp$ lin light-field configuration and $J_g = 1 \to J_e = 2$ under $\sigma^+\sigma^-$ configuration equations for the coefficients of diffusion D and friction ξ were found in Ref. [63] (for arbitrary laser-field configuration the equations were derived in Ref. [67]). Figure 9 shows the profile of function β for magnesium atom and transition $J_g = 2 \to J_e = 3$. It means that at certain saturation parameter (intensity of light field) for considering frequency detuning region the temperature of atoms under lin $\perp$ lin configuration is always noticeably lower than under $\sigma^+\sigma^-$ field. Nevertheless, it should be noted that with small saturation parameters the linear dependence of temperature (35) is valid only for slow atomic velocity assumption (34). Combining (34) and (35) we come to the new requirement

$$\frac{\hbar k^2}{\gamma M}\beta \ll S_0\,, \tag{36}$$

that leads to severe limitation in the case of small saturation parameters ($S_0 < 1$)

$$\tilde{\omega}_{\rm rec}\beta \ll S_0, \tag{37}$$

where dimensionless recoil frequency $\tilde{\omega}_{\rm rec} = \omega_{\rm rec}/\gamma$. This new strict requirement is similar to the semiclassical condition (1), and it must be satisfied to make the semiclassical approach valid [60].

In case of magnesium, the parameter $\omega_{\rm rec}/\gamma$ can be not small enough to satisfy the strict requirement (37) and, therefore, Eq. (35) can be inadequate for estimating the temperature. In this case, the full (nonlinear) dependence of diffusion coefficient and radiation force on the atomic velocity must be taken into account. Then, in general, steady-state velocity distribution is not just Gaussian type and should be defined via the equation [54]

$$f(\tilde{\upsilon}) = \frac{\rm const}{\langle D(\tilde{\upsilon})\rangle_z}\exp\left[\int_{-\infty}^{\tilde{\upsilon}}\frac{\langle F(\tilde{\upsilon}')\rangle_z}{2\omega_{\rm rec}\langle D(\tilde{\upsilon}')\rangle_z}d\tilde{\upsilon}'\right]. \tag{38}$$

Here, radiation force F and diffusion coefficient D are defined by $\hbar k\gamma$ and $(\hbar k)^2\gamma$, respectively, $\tilde{\upsilon}$ is the dimensionless Doppler shift $k\upsilon/\gamma$. In the one-dimensional case the corresponding effective temperature can be found from the following equation:

$$T_{\rm eff}/T_{\rm rec} = \frac{1}{4\tilde{\omega}_{\rm rec}}\int_{-\infty}^{+\infty}\tilde{\upsilon}^2 f(\tilde{\upsilon})d\tilde{\upsilon}\,, \tag{39}$$

where $T_{\rm rec} = 2\hbar\omega_{\rm rec}/k_B$ is the recoil temperature.

As one can see, function β is much larger for the $\sigma^+\sigma^-$ field than for the lin $\perp$ lin one. It means that linear regime (35) for certain saturation parameter S_0 may be justified for the lin $\perp$ lin field, showing sub-Doppler temperatures, and may be not valid for the $\sigma^+\sigma^-$ field, that results in much higher temperatures in the last case. In other words, light magnesium atoms, having not enough small recoil frequency $\omega_{\rm rec}$, do not feel influence of sub-Doppler mechanism on the friction force, and the cooling process is determined mainly by regular Doppler cooling mechanism under counterpropagating waves.

IV. CONCLUSION

In conclusion, we would like to summarize the main results of our work. We have suggested using the second

sub-Doppler cooling stage to solve the problem of deep laser cooling of magnesium atoms. The first stage implies using a regular magneto-optical trap involving dipole transition between triplet states $3\,^3P_2$ and $3\,^3D_3$. In particular, this stage was used in the experiment of researches from Hannover University [46]. In spite of the level $3\,^3P_2$ is degenerate and one could anticipate activation of effective sub-Doppler mechanism of cooling under polarization-gradient field [63], however, conducted theoretical analysis (in 1D) has figured out the minimum temperature at the level of 310 μK, which is just a little bit lower than the estimate for Doppler limit of cooling ($T_D \approx 425\ \mu$K). To reduce this value by several times we have proposed and analyzed the second laser-cooling stage involving an optical molasses composed of two counterpropagating orthogonally linearly polarized waves (lin $\perp$ lin field configuration). In contrast to the $\sigma^+\sigma^-$ field, usually applied in a MOT, the optical molasses can provide much lower temperature (80 μK). At the same time, the minimum achievable temperature of laser cooling in the case of ^{24}Mg still is noticeably higher than for some other atoms, where sub-Doppler mechanism brought much better results. It is most likely due to relatively large recoil energy of magnesium atom. For instance, for considered transition in magnesium recoil frequency $\omega_{\rm rec} \approx 2\pi \times 53$ kHz, while for ^{133}Cs ($^2S_{1/2}$, $F = 4 \rightarrow {}^2P_{3/2}$, $F = 5$) this frequency is significantly smaller ($\omega_{\rm rec} \approx 2\pi \times 2$ kHz), that allowed cooling cesium atoms down to 2.5 μK [68].

Aside from temperature (average kinetic energy) of the atomic ensemble, we have also paid attention to the linear momentum distributions in the steady state. In particular, we have investigated the problem of increasing concentration of atoms in the ultracold fraction (a region in momentum space in the vicinity of $p = 0$). Conducted numerical calculations have revealed the optimum parameters of laser field to maximize the ultracold fraction ($T_{\rm eff} \sim 1\ \mu$K). This fraction can be easily localized in the shallow optical trap, while the other fraction ("hot" atoms) can be removed from the trap by proper choice of the optical depth (it can be called as "cooling" by selection of atomic velocities). At that, it is the second stage of sub-Doppler cooling to provide great increase of ultracold atomic number in comparison with the case when only the first stage has been implemented (e.g., as in the experiments [33,34,46]).

In our theoretical analysis, quantum treatment has been exploited with taking into account the recoil effect, i.e., we have not been limited by semiclassical or secular approximations as well as a weak-field limit. It has allowed us to study kinetics of cold magnesium in a wide range of intensity and frequency detuning to determine the optimum parameters of a laser field. Also, we have compared data provided by quantum and semiclassical approaches. As a result, we can conclude that the semiclassical approach in case of transition $3\,^3P_2 \rightarrow 3\,^3D_3$ in ^{24}Mg is not valid for an adequate understanding of the kinetics of ultracold magnesium atoms for a wide range of light-field parameters. Moreover, we can also conclude that to get an adequate estimate of cooling parameters and understand the problems of deep laser cooling of magnesium atoms, it is quite necessary to treat the problems with the help of a quantum approach.

In the end, we should note that in spite of the fact that a theoretical analysis has been performed beyond many widely used approximations, we have assumed the problem to be one dimensional. However, light-field configuration used in a magneto-optical trap is always three dimensional (three pairs of circularly polarized beams). Therefore, obviously, the results of such 1D analysis may differ from the real experiment with a 3D field. For example, one can refer to the papers [69,70] for getting the estimate of such kind of difference. In these papers, calculations were made for 1D and 3D configurations by the example of simple transition $F_g = 0 \rightarrow F_e = 1$ under limits of semiclassical and slow-atoms approximations. At the same time, an optical molasses (the second cooling stage suggested), which is the most interesting from the viewpoint of deep laser cooling, can be implemented both in 3D and 1D configurations. Three-dimensional optical molasses for various transitions of the type $F_g = F \rightarrow F_e = F + 1$ was investigated in Ref. [71] under weak-saturation approximation and with the help of adiabatic reduction of density matrix equations to the ground state. Unfortunately, that approximation does not give good results for a wide range of light-field intensity and frequency detuning that are of a great interest to laser cooling (e.g., see the work [64], where the results of adiabatic approximation were compared to the results of a full quantum treatment). Three-dimensional quantum treatment with a full account of the recoil effect and beyond the aforesaid approximations is quite challenging and requires to be studied separately.

ACKNOWLEDGMENT

The work was partially supported by the Ministry of Education and Science of the Russian Federation (Gov. Order No. 2014/139, Project No. 825), Presidium of the Siberian Branch of the Russian Academy of Sciences, and by the grants of RFBR (Grants No. 15-02-06087, No. 15-32-20330, No. 14-02-00806, No. 14-02-00712, No. 14-02-00939) and Russian Presidential grants (Grants No. MK-4680.2014.2 and No. NSh-4096.2014.2).

[1] F. Riehle, *Frequency Standards: Basics and Applications* (Wiley, Weinheim, 2004).

[2] A. D. Ludlow *et al.*, Science **319**, 1805 (2008).

[3] P. Komar, E. M. Kessler, M. Bishof, L. Jiang, A. S. Sorensen, J. Ye, and M. D. Lukin, Nat. Phys. **10**, 582 (2014).

[4] T. Akatsuka, H. Ono, K. Hayashida, K. Araki, M. Takamoto, T. Takano, and H. Katori, Jpn. J. Appl. Phys. **53**, 032801 (2014).

[5] G. Marra, J. Kronjaeger, P.-E. Pottie *et al.*, in the electronic *Book of Abstracts of 28th European Frequency and Time Forum, Neuchatel, Switzerland, 2014* (The Printing House Inc., Stoughton, 2014), p. 164.

[6] M. Takamoto, I. Ushijima, M. Das *et al.*, C. R. Phys. (to be published).

[7] M. Takamoto, F.-L. Hong, R. Higashi, and H. Katori, Nature (London) **435**, 321 (2005).

[8] P. Lemonde, Eur. Phys. J. Spec. Top. **172**, 81 (2009).

[9] A. P. Kazantsev, G. I. Surdutovich, and V. P. Yakovlev, *Mechanical Action of Light on Atoms* (World Scientific, Singapore, London, 1990).

[10] H. Katori, in *Proceedings of the 6th Symposium on Frequency Standards and Metrology, University of St. Andrews, Fife, Scotland, 2001*, edited by P. Gill (World Scientific, Singapore, 2002).

[11] H. Katori, M. Takamoto, V. G. Pal'chikov, and V. D. Ovsiannikov, Phys. Rev. Lett. **91**, 173005 (2003).

[12] M. Takamoto and H. Katori, Phys. Rev. Lett. **91**, 223001 (2003).

[13] C. W. Hoyt, Z. W. Barber, C. W. Oates, T. M. Fortier, S. A. Diddams, and L. Hollberg, Phys. Rev. Lett. **95**, 083003 (2005).

[14] T. Hong, C. Cramer, E. Cook, W. Nagourney, and E. N. Fortson, Opt. Lett. **30**, 2644 (2005).

[15] M. Petersen, R. Chicireanu, S. T. Dawkins, D. V. Magalhães, C. Mandache, Y. Le Coq, A. Clairon, and S. Bize, Phys. Rev. Lett. **101**, 183004 (2008).

[16] V. I. Yudin, A. V. Taichenachev, C. W. Oates, Z. W. Barber, N. D. Lemke, A. D. Ludlow, U. Sterr, Ch. Lisdat, and F. Riehle, Phys. Rev. A **82**, 011804 (2010).

[17] H. Katori, Nat. Photonics **5**, 203 (2011).

[18] S. Falke, N. Lemke, Ch. Grebing *et al.*, New J. Phys. **16**, 073023 (2014).

[19] B. J. Bloom, T. L. Nicholson, J. R. Williams, S. L. Campbell, M. Bishof, X. Zhang, W. Zhang, S. L. Bromley, and J. Ye, Nature (London) **506**, 71 (2014).

[20] I. Ushijima, M. Takamoto, M. Das, T. Ohkubo, and H. Katori, Nat. Photonics **9**, 185 (2015).

[21] Z. W. Barber, C. W. Hoyt, C. W. Oates, L. Hollberg, A. V. Taichenachev, and V. I. Yudin, Phys. Rev. Lett. **96**, 083002 (2006).

[22] N. Hinkley, J. A. Sherman, N. B. Phillips, M. Schioppo, N. D. Lemke, K. Beloy, M. Pizzocaro, C. W. Oates, and A. D. Ludlow, Science **341**, 1215 (2013).

[23] N. D. Lemke, A. D. Ludlow, Z. W. Barber, T. M. Fortier, S. A. Diddams, Y. Jiang, S. R. Jefferts, T. P. Heavner, T. E. Parker, and C. W. Oates, Phys. Rev. Lett. **103**, 063001 (2009).

[24] C. Degenhardt, H. Stoehr, U. Sterr, F. Riehle, and Ch. Lisdat, Phys. Rev. A **70**, 023414 (2004).

[25] T. Akatsuka, M. Takamoto, and H. Katori, Phys. Rev. A **81**, 023402 (2010).

[26] J. J. McFerran, L. Yi, S. Mejri, S. Di Manno, W. Zhang, J. Guena, Y. Le Coq, and S. Bize, Phys. Rev. Lett. **108**, 183004 (2012).

[27] J. Friebe, M. Riedmann, T. Wübbena, A. Pape, H. Kelkar, W. Ertmer, O. Terra, U. Sterr, S. Weyers, G. Grosche, H. Schnatz, and E. M. Rasel, New J. Phys. **13**, 125010 (2011).

[28] A. N. Goncharov *et al.*, Quantum Electron. **44**, 521 (2014).

[29] A. V. Taichenachev, V. I. Yudin, C. W. Oates, C. W. Hoyt, Z. W. Barber, and L. Hollberg, Phys. Rev. Lett. **96**, 083001 (2006).

[30] T. Akatsuka, M. Takamoto, and H. Katori, Nat. Phys. **4**, 954 (2008).

[31] T. Legero, C. Lisdat, J. S. R. Vellore Winfred *et al.*, IEEE Trans. Instrum. Meas. **58**, 1252 (2009).

[32] N. Poli, M. Schioppo, S. Vogt, St. Falke, U. Sterr, Ch. Lisdat, and G. M. Tino, Appl. Phys. B **117**, 1107 (2014).

[33] E. M. Rasel *et al.*, in the electronic *Book of Abstracts of the 28th International Frequency and Time Forum, Neuchatel, Switzerland, 2014* (The Printing House Inc., Stoughton, 2014), p. 138.

[34] A. P. Kulosa, D. Fim, K. H. Zipfel, S. Rühmann, S. Sauer, N. Jha, K. Gibble, W. Ertmer, E. M. Rasel, M. S. Safronova, U. I. Safronova, and S. G. Porsev, arXiv:1508.01118v1.

[35] Y. Takasu, K. Maki, K. Komori, T. Takano, K. Honda, M. Kumakura, T. Yabuzaki, and Y. Takahashi, Phys. Rev. Lett. **91**, 040404 (2003).

[36] S. Kraft, F. Vogt, O. Appel, F. Riehle, and U. Sterr, Phys. Rev. Lett. **103**, 130401 (2009).

[37] S. Stellmer, M. K. Tey, Bo Huang, R. Grimm, and F. Schreck, Phys. Rev. Lett. **103**, 200401 (2009).

[38] T. E. Mehlstäubler, K. Moldenhauer, M. Riedmann, N. Rehbein, J. Friebe, E. M. Rasel, and W. Ertmer, Phys. Rev. A **77**, 021402 (2008).

[39] N. Rehbein, T. E. Mehlstäubler, J. Keupp *et al.*, Phys. Rev. A **76**, 043406 (2007).

[40] See http://physics.nist.gov/asd.

[41] S. Rühmann, A. Kulosa, D. Fim, K. Zipfel, W. Ertmer, and E. Rasel, in the electronic *Book of Abstracts of the 28th International Frequency and Time Forum, Neuchatel, Switzerland, 2014* (The Printing House Inc., Stoughton, 2014), p. 213.

[42] S. G. Porsev and A. Derevianko, Phys. Rev. A **74**, 020502 (2006).

[43] H. Hachisu, K. Miyagishi, S. G. Porsev, A. Derevianko, V. D. Ovsiannikov, V. G. Pal'chikov, M. Takamoto, and H. Katori, Phys. Rev. Lett. **100**, 053001 (2008).

[44] F. Y. Loo, A. Brusch, S. Sauge, M. Allegrini, E. Arimondo, N. Andersen, and J. W. Thomsen, J. Opt. B **6**, 81 (2004).

[45] J. Keupp *et al.*, Eur. Phys. J. D **36**, 289 (2005).

[46] M. Riedmann, H. Kelkar, T. Wübbena, A. Pape, A. Kulosa, K. Zipfel, D. Fim, S. Rühmann, J. Friebe, W. Ertmer, and E. Rasel, Phys. Rev. A **86**, 043416 (2012).

[47] S. Stellmer, R. Grimm, and F. Schreck, Phys. Rev. A **87**, 013611 (2013).

[48] G. Santarelli, Ph. Laurent, P. Lemonde, A. Clairon, A. G. Mann, S. Chang, A. N. Luiten, and C. Salomon, Phys. Rev. Lett. **82**, 4619 (1999).

[49] J. Dalibard *et al.*, J. Phys. B: At., Mol. Opt. Phys. **17**, 4577 (1984).

[50] T. Binnewies, G. Wilpers, U. Sterr, F. Riehle, J. Helmcke, T. E. Mehlstäubler, E. M. Rasel, and W. Ertmer, Phys. Rev. Lett. **87**, 123002 (2001).

[51] E. A. Curtis, C. W. Oates, and L. Hollberg, Phys. Rev. A **64**, 031403 (2001).

[52] H. Katori, T. Ido, Y. Isoya, and M. Kuwata-Gonokami, Phys. Rev. Lett. **82**, 1116 (1999).

[53] T. Kuwamoto, K. Honda, Y. Takahashi, and T. Yabuzaki, Phys. Rev. A **60**, R745(R) (1999).

[54] D. V. Brazhnikov, A. E. Bonert, A. N. Goncharov, A. V. Taichenachev, and V. I. Yudin, Laser Phys. **24**, 074011 (2014).

[55] V. G. Minogin and V. S. Letokhov, *Laser Light Pressure on Atoms* (Gordon and Breach, New York, 1987).

[56] Y. Castin, H. Wallis, and J. Dalibard, J. Opt. Soc. Am. B **6**, 2046 (1989).

[57] A. P. Kazantsev, V. S. Smirnov, G. I. Surdutovich, D. O. Chudesnikov, and V. P. Yakovlev, J. Opt. Soc. Am. B **2**, 1731 (1985).

[58] V. G. Minogin, Zh. Eksp. Teor. Fiz. **79**, 2044 (1980) [J. Exp. Theor. Phys. **52**, 1032 (1980)].

[59] R. J. Cook, Phys. Rev. A **22**, 1078 (1980).

[60] J. Dalibard and C. Cohen-Tannoudji, J. Phys. B: At. Mol. Phys. **18**, 1661 (1985).

[61] J. Javanainen, Phys. Rev. A **44**, 5857 (1991).
[62] F. Svensson, S. Jonsell, and C. M. Dion, Eur. Phys. J. D **48**, 235 (2008).
[63] J. Dalibard and C. Cohen-Tannoudji, J. Opt. Soc. Am. B **6**, 2023 (1989).
[64] O. N. Prudnikov, R. Ya. Il'enkov, A. V. Taichenachev, A. M. Tumaikin, and V. I. Yudin, J. Exp. Theor. Phys. **112**, 939 (2011).
[65] D. A. Varshalovich, A. N. Moskalev, and V. K. Khersonskii, *Quantum Theory of Angular Momentum* (World Scientific, Singapore, 1989).
[66] A. V. Taichenachev, A. M. Tumaikin, and V. I. Yudin, Laser Phys. **2**, 575 (1992).
[67] A. V. Bezverbnyi, O. N. Prudnikov, A. V. Taichenachev, A. M. Tumaikin, and V. I. Yudin, J. Exp. Theor. Phys. **96**, 383 (2003).
[68] C. Salomon, J. Dalibard, W. D. Phillips, A. Clairon, and S. Guellati, Europhys. Lett. **12**, 683 (1990).
[69] S.-K. Choi, S. E. Park, J. Chen, and V. G. Minogin, Phys. Rev. A **77**, 015405 (2008).
[70] O. N. Prudnikov, A. V. Taichenachev, and V. I. Yudin, Zh. Eksp. Teor. Fiz. **147**, 678 (2015) [J. Exp. Theor. Phys. **120**, 587 (2015)].
[71] Y. Castin and K. Molmer, Phys. Rev. Lett. **74**, 3772 (1995).